Fabrication of hybrid metal systems through the application of high-pressure torsion

Megumi Kawasaki[1,2,*], Dae-Kuen Han[1], Jae-Kyung Han[1], Jae-il Jang[1], Terence G Langdon[2,3]

[1]Division of Materials Science and Engineering, Hanyang University, Seoul 133-791, South Korea
[2]Departments of Aerospace & Mechanical Engineering and Materials Science, University of Southern California, Los Angeles, CA 90089-1453, U.S.A.
[3]Materials Research Group, Faculty of Engineering and the Environment, University of Southampton, Southampton SO17 1BJ, U.K.

*megumi@hanyang.ac.kr

Abstract. This presentation demonstrates a simple and very rapid synthesis of metal matrix nanocomposites (MMNCs) in Al-based hybrid systems which are achieved by processing stacked disks of two pure metals through the application of high-pressure torsion (HPT) at ambient temperature. These synthesized hybrid systems exhibit exceptionally high hardness through rapid deformation-induced diffusion and the simultaneous formation of different intermetallic compounds. The experiments also show further improvement in mechanical properties is available by increasing the numbers of HPT turns and additional short-term annealing. Thus, by demonstrating the fabrication of the Al-Mg and Al-Cu hybrid systems, the present paper suggests a potential for simply and expeditiously fabricating a wide range of MMNCs through HPT.

1. Introduction

The light-weight metals including aluminum, magnesium and cupper are widely used for structural applications in the automotive, aerospace and electronic industries but improvements in the mechanical properties of these metals would be attractive for enhancing their future use. In practice, an earlier study on an aerospace-grade Al-7075 alloy reported an increase in the strength limit of the alloy by processing using high-pressure torsion (HPT) while maintaining reasonable formability [1]. Nevertheless, it is reasonable to anticipate that there is probably an upper limit in the maximum achievable mechanical properties when the processing is conducted directly on the alloy. This suggests a new strategy for achieving superior properties of materials by bonding dissimilar metals and synthesizing new metal systems.

Bulk nanostructured materials with ultrafine grains (UFG) can be fabricated through the application of severe plastic deformation (SPD) which is a promising technique for achieving significant grain refinement in bulk metals [2]. Among the reported SPD techniques, one of the most attractive methods refers to processing by HPT where this type of processing leads to exceptional grain refinement that is not generally achieved using other procedures [3]. The processed metals generally demonstrate an enhancement in the physical and mechanical characteristics through significant grain refinement at room temperature (RT) and the intensive introduction of point and line defects [4]. Because of the introduction of intense plastic straining during processing, HPT has been applied also for the bonding of machining chips [5,6] and the consolidation of metallic powders [7-9].

Accordingly, a new approach of applying conventional HPT processing was studied for the formation of Al-Mg and Al-Cu hybrid systems and ultimately attaining a metal matrix nanocomposite (MMNC) from separate Al, Mg and Cu disks through diffusion bonding at RT under high pressure. Specifically, the present reports describe the unique microstructure, hardness distributions and the micro-mechanical response for an Al-Mg hybrid system synthesized by HPT. A study of post-deformation annealing (PDA) was applied to demonstrate the improvement in plasticity by an increase in the strain rate sensitivity, *m*, in the synthesized alloy system. Moreover, the feasibility of the HPT processing in the preparation of new alloy systems is demonstrated by forming an Al-Cu alloy system recording very high hardness due to significant grain refinement during HPT.

2. Fabrication of an Al-Mg hybrid system

A commercial purity Al-1050 alloy and a ZK60 magnesium alloy were used for the experiments. The extruded bars of the alloys having a diameter of 10 mm were cut into billets with lengths of ~65 mm and a number of disks was sliced from the billets and polished to achieve uniform thicknesses of ~0.83 mm. The direct bonding of the Al and Mg disks was performed through the conventional HPT procedure at RT using a quasi-constrained facility under a hydraulic pressure of 6.0 GPa for 1, 5, 10 and 20 turns at a rotational speed of 1 rpm. In particular, a set of the separate Al and Mg disks were placed in the depression on the lower anvil in the order of Al/Mg/Al where the Mg disk was positioned between the two Al disks but without using any glue or metal brushing treatment. A schematic illustration of the sample set-up between the conventional HPT anvils is shown in Figure 1(a) [10,11].

Figure 1(b) shows overviews of the microstructure taken at the cross-sections of the Al-Mg disks by optical microscopy (OM) after HPT for 1, 5 and 10 turns from the top, respectively, where the bright regions denote the Al-rich phase and the dark regions correspond to the Mg-rich phase in these micrographs [10-12].

A disk after 1 turn by HPT showed a multi-layered structure with fragmented Mg layers with thicknesses of ~200 µm without any segregation of Al and Mg phases throughout the disk diameter. A similar microstructure consisting of multi-layers of the Al and Mg phases was observed at the central regions at r <2.0 and <1.0 mm of the disks after 5 and 10 turns, respectively, where r denotes the radius of the HPT disk. However, the disk peripheries at r >2.5 mm after 5 turns demonstrated a unique microstructure involving a homogeneous distribution of very fine Mg phases having thicknesses of ~5-10 µm to even true nano-scale sizes of ~100-500 nm within the Al matrix. Furthermore, the Mg phases disappeared at the disk edge and thus there was no evidence of visible Mg phases at ~3< r <5 mm after 10 turns.

The distributions of Vickers microhardness was examined over the vertical cross-sections of the processed disks and the data set was visualized by constructing color-coded hardness contour maps as shown in Figure 1(c) for 1, 5 and 10 turns from the top, respectively, where the hardness values are indicated in the key on the right. For reference, the Al-1050 alloy and the ZK60 alloy show a saturation hardness of Hv ≈ 65 and ~110 across the disk diameters after HPT for 5 turns providing sufficient torsional straining.

The total cross-section after HPT for 1 turn shows an average microhardness value of ~70. This is similar to the value of ~65 for the base material of the Al-1050 alloy after HPT for 5 turns and this hardness value remains constant at the centers at r <2.5 mm of the Al-Mg disks up to 10 turns. However, additional HPT turns to 5 introduced high hardness with a maximum of Hv ≈ 130 in the peripheral region where the fine Mg phase is homogeneously distributed within the Al matrix. Moreover, there is a significant increase in Hv after 10 turns where a maximum hardness of ~270 was recorded at the peripheral region at r >3.0 mm. These high hardness values measured in the Al-Mg system after HPT are much higher than the base alloys of Al and Mg after HPT and a detailed microstructural analysis is necessary to understand the hardening mechanism of this unique Al-Mg system produced by HPT processing.

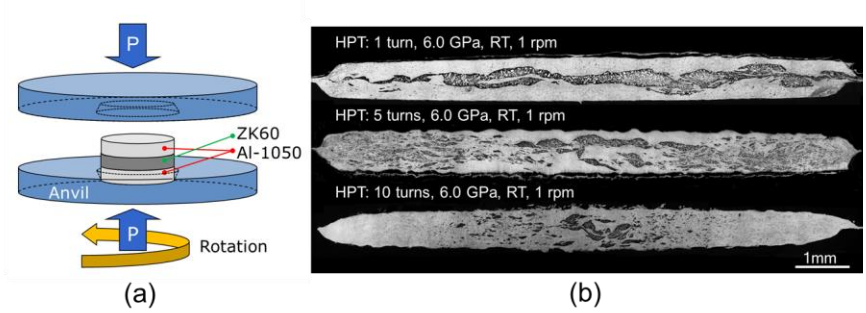

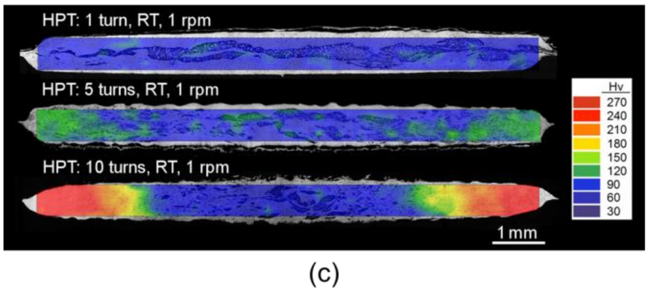

Figure 1. (a) Schematic illustration of the sample set-up for HPT processing and (b) an overview of the microstructure and (c) color-coded hardness contour maps taken at the vertical cross-sections along the disk diameters after HPT for 1, 5 and 10 turns, respectively [10-12].

Processing by HPT was continued up to 20 turns to evaluate the possibility of achieving further improvement in hardness. Moreover, PDA at 573 K for 1 hour was applied to investigate the change in microstructure and the enhancement in mechanical properties in the Al-Mg alloy system. There are several recent reports demonstrating the significance of PDA on the mechanical properties at RT of HPT-processed materials [13-15]. Microstructures taken at the vertical cross-sections and the color-coded hardness contour maps are shown in Figure 2(a) and (b), respectively, for the Al-Mg disks after HPT at RT for 20 turns (upper) and after HPT followed by PDA at 573 K for 1 hour (lower) [16].

It is apparent that the deformed microstructure after HPT for 20 turns is reasonably similar to the sample conditions in the Al-Mg system after HPT for 10 turns as shown in Figure 1(b) where there are multi-layered Al and Mg phases at the disk center but there is a complete dissolution of Mg in the Al matrix. A similar microstructure was observed after PDA whereas the outer region involving the complete mixture of Mg within Al was reduced. Accordingly, the synthesized Al-Mg system after HPT and after PDA consists of gradient-type microstructures across the disk diameters.

There is a drastic increase in hardness in the Al-Mg disk after HPT for 20 turns. Specifically, a Vickers microhardness of Hv ≈ 60 and slightly higher was observed at the central region of the disk at $r < 2.5$ mm and then a transition in hardness to ~150-240 was measured at $r \approx 2.5$-3.5 mm followed by an exceptionally high hardness of Hv ≈ 330 at $r \approx 4.0$-5.0 mm. This high hardness is significantly higher than the highest value of Hv ≈ 270 observed in the Al-Mg disk processed by HPT for 10 turns as shown in Figure 1(c). After PDA, there was a slight reduction in hardness to Hv ≈ 30 in the central regions up to $r \approx 3.0$ mm and a reduction to Hv ≈ 220 at the outer region of the disk at $r \approx 4.0$-5.0 mm. Thus, the changes in microstructure correlate directly with the values of hardness in the Al-Mg system after HPT and there is a significant hardness variation in the synthesized Al-Mg through the HPT processing. Accordingly, the detailed microstructures at the disk peripheries demonstrating exceptional hardness were examined by TEM and the microstructures are displayed in Figure 3 for the samples after (a)-(b) 20 HPT turns and (c) HPT followed by PDA. In addition, the XRD profiles for these two samples are demonstrated in Figure 3(d) and (e), respectively.

As seen in Figure 3(a) and (b), there is a mixture of regions with a layered structure and an equiaxed microstructure at the disk edge immediately after HPT for 20 turns. In practice, the layered microstructure has an average thickness of ~20 nm and these layers contain numerous dislocations which subdivide the layers in a vertical sense. The equiaxed grains showed an average grain size of $d \approx 60$ nm. By contrast, it is apparent from Figure 3(c) that after PDA the HPT-processed Al-Mg system contained a homogeneous equiaxed microstructure with an average grain size of $d \approx 380$ nm.

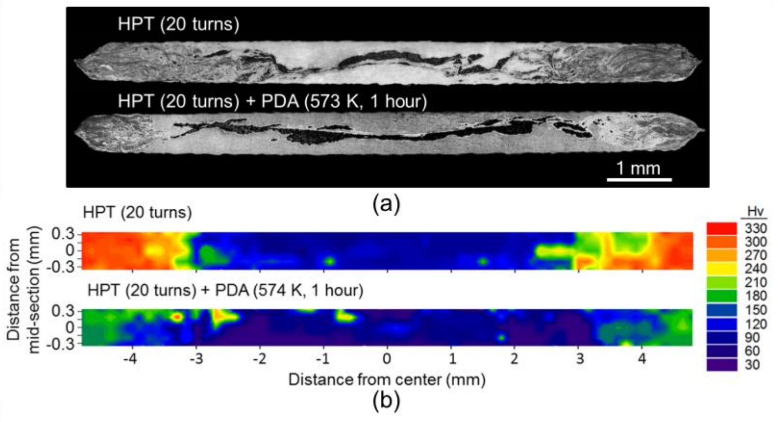

Figure 2. (a) The OM micrographs of the Al-Mg disks after HPT at room temperature under a pressure of 6.0 GPa and (b) color-coded contour maps of the Vickers microhardness for the vertical cross-sectional planes after HPT for 20 turns (upper) and after HPT and PDA (lower), respectively. [16]

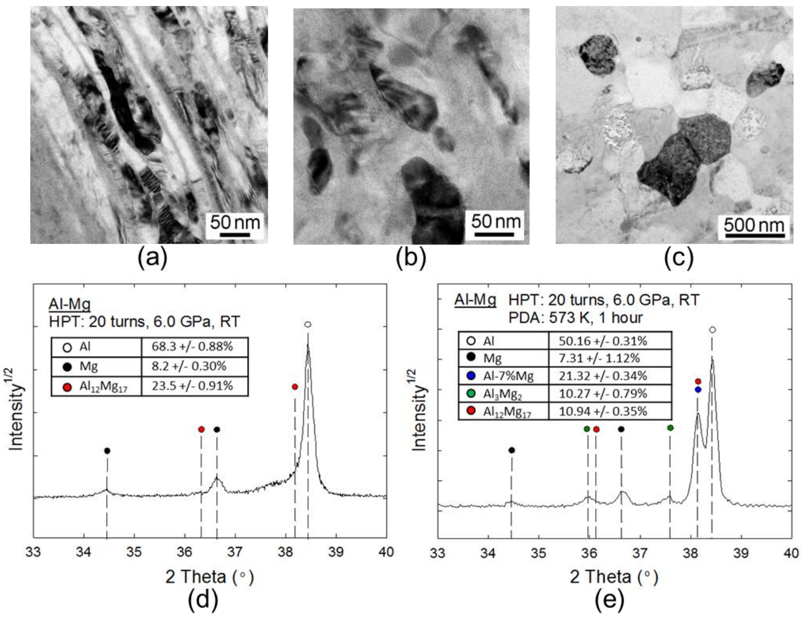

Figure 3. Representative TEM bright-field images taken at the disk edges after (a)-(b) HPT for 20 turns and (c) HPT followed by PDA in the Al-Mg system and the X-ray diffraction profiles for the disk edges of the Al-Mg system after (d) HPT for 20 turns and (e) HPT and PDA [16].

The results of the X-ray analysis are shown in Figure 3 (d) and (e) where additional compositional analysis based on the X-ray profile through MOUD was displayed as a table in each plot. It should be noted that the samples at the disk edges were carefully prepared by removing the central regions so that the measurements focused only on the peripheral regions where Mg was completely dissolved into the Al matrix after HPT for 20 turns and after PDA as seen in Figure 2 whereas the inevitable concentrations of the Mg-rich phase existed close to the mid-radius of the processed samples.

The disk edge immediately after HPT for 20 turns showed there is evidence of a γ-$Al_{12}Mg_{17}$ intermetallic compound in the Al matrix whereas after PDA there is an Al-7% Mg solid solution phase with two different β-Al_3Mg_2 and γ-$Al_{12}Mg_{17}$ intermetallic compounds. Thus, it is established that processing by HPT for 20 turns and additional PDA produced two different types of deformation-induced MMNCs containing intermetallic compounds at the disk edges of the Al-Mg system.

The synthesis of intermetallic compounds at RT is feasible due to the accelerated diffusivity of Mg atoms into the Al matrix that is attributed to SPD under high pressure [10]. Several recent studies demonstrated experimental evidence for enhanced atomic diffusion in nanostructured materials processed by ECAP [17] and HPT [10,18]. Moreover, a recent review describes the significance of the fast atomic mobility during SPD by recognizing the significant increase in the vacancy concentration through SPD processing [19]. Accordingly, the present experimental results also anticipate that the formation of these intermetallic compounds provides an excellent potential for reinforcing the Al matrix by improving the hardness and strength.

3. Micro-mechanical response of the MMNCs in the Al-Mg system

The micro-mechanical response was examined by applying the nanoindentation technique for the disk edges consisting of MMNCs in the Al-Mg system after HPT for 20 turns and subsequent PDA. The analysis used a nanoindentation facility, Nanoindenter-XP (formerly MTS; now Agilent, Oak Ridge, TN) with a three-sided pyramidal Berkovich indenter having a centerline-to-face angle of 65.3°. More than 15 indentations were conducted at each specific phase at the measured locations to provide statistically valid data. All measurements were conducted under a predetermined peak applied load of P_{max} = 50 mN at constant indentation strain rates of 0.0125, 0.025, 0.05 and 0.1 s^{-1} which are equivalent to general strain rates of 1.25×10^{-4}, 2.5×10^{-4}, 5.0×10^{-4} and 1.0×10^{-3} s^{-1} calculated through an empirical relationship [20].

Figure 4 shows representative load-displacement curves for the Al-Mg disk edges after (a) HPT for 20 turns and (b) HPT and PDA when measuring at four strain rates [16]. The disk edge after HPT for 20 turns demonstrated no strain rate dependency where all four load-displacement curves placed in reasonably consistent locations as shown in Figure 4(a). However, there is a slight tendency of less displacement when the strain rate is slower, thereby indicating a negative strain rate dependency of plasticity. By contrast, the Al-Mg system after HPT followed by PDA demonstrated an apparent positive strain rate dependency where increasing displacements were achieved at slower strain rates of nanoindentation as shown in Figure 4(b). It is also apparent by comparing the load-displacement curves between the two samples that the MMNC immediately after HPT shows much lower displacements than the MMNC after HPT and PDA at all strain rates, thereby demonstrating the high hardness of the MMNC in the Al-Mg disk edge immediately after HPT for 20 turns. This result is fully consistent with the Vickers hardness measurements as shown in Figure 2(b).

Considering Tabor's empirical prediction where the flow stress is equivalent to one-third of hardness, H, measured through nanoindentaion testing for fully-plastic deformation at a constant strain rate, the strain rate sensitivity, *m*, was determined from the slope of the line for each examined sample in a logarithmic plot of H/3 against the strain rate as shown in Figure 4(c) for the disk edges of the Al-Mg system after HPT for 20 turns and after HPT followed by PDA [16].

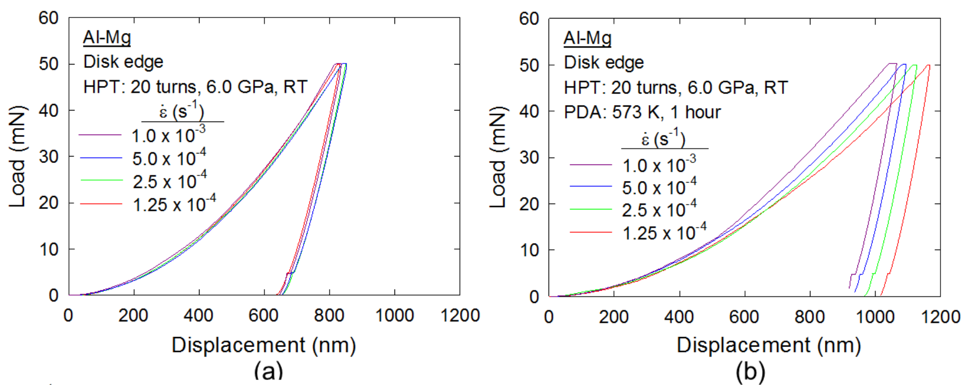

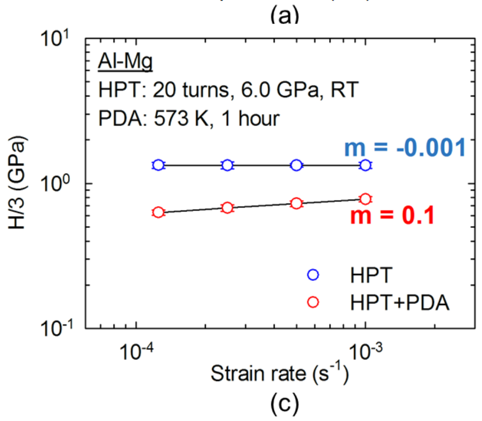

Figure 4. Representative load-displacement curves for the Al-Mg disk edges after (a) HPT for 20 turns and (b) HPT and PDA when measuring at four strain rates at 1.0×10^{-3} - 1.25×10^{-4} s^{-1} under a predetermined maximum peak load of 50 mN and (c) variations in the strain rate sensitivity with increasing strain rate for the disk edges of the Al-Mg system after HPT for 20 turns and after HPT and PDA [16].

The analysis estimated the *m* values of –0.001 and 0.1 for the MMNCs at the Al-Mg disk edges immediately after HPT and after HPT followed by PDA, respectively. It has been well described that there is generally a significant loss of ductility in bulk nanostructured materials where a marked increase in hardness and strength is achieved by grain refinement through SPD [21-23]. Specifically, the lower overall ductility in the UFG materials is attributed to an inter-relationship between the lower strain hardening and an increasing strain rate sensitivity [24,25]. Nevertheless, the present nanoindentation analysis shows that there is a significant increase in the strain rate sensitivity in the HPT-induced MMNC after PDA. Thus, a PDA treatment is a feasible procedure for enhancing the RT plasticity in the MMNC in the Al-Mg hybrid system synthesized by HPT while maintaining reasonably high hardness as shown in Figure 2(b).

The significance of PDA was demonstrated earlier for improving the overall ductility of nanostructured Ti after HPT [13]. A recent review demonstrated that a PDA treatment produces an ordering of the defect structures within the grain boundaries leading to an equilibrium state without any significant grain growth [23]. In addition, short-term annealing reduces the dislocation density in the grain interior of the UFG material after SPD so that the dislocation storage capability may increase and thus the strain hardening capability is enhanced leading to the possibility of high ductility in the SPD-processed material. Accordingly, by the addition of a PDA treatment, the MMNC in the Al-Mg system produced by HPT has a great potential for demonstrating both high hardness and superior ductility.

4. Future potential of the HPT technique for synthesizing new metal systems

There are only limited numbers of demonstrations to date of the fabrication of hybrid material showing high mechanical performance by bonding dissimilar bulk metals to form new metal systems through HPT. A first report demonstrated a solid-state reaction in an Al-Cu system through the bonding of semi-circular half-disks of commercial purity Al and Cu using HPT at ambient temperature for up to 100 turns [26]. Thereafter, a similar approach was applied for forming a spiral texture by processing of an Al-Cu hybrid material though HPT where four quarter-disks, including two of pure Cu and two of an Al-6061 alloy, were positioned to make a complete disk and then processed by HPT at RT for 1 turn [27]. However, this study described only the computational calculation of the distribution of equivalent stress in the processed Al-Cu disk using a finite element method and there was no detailed microstructural analysis of the processed disk.

Accordingly, a simpler approach for utilizing conventional HPT processing for the bonding of separate Al and Mg disks was processed by stacking a set of two disks for up to 20 turns [28] and stacking three disks for 5-10 turns [10-12] and for 20 turns [16] for producing bi-layered and multi-layered structures, respectively, in an Al-Mg system through HPT at RT. It should be emphasized that the MMNCs synthesized at the disk edges of the Al-Mg system receive very high straining through HPT but in the present study the final bulk metal contains a gradient-type microstructure or a heterogeneous nanostructure which involves gradations of not only grain size but also compositions [29]. This is a new category of bulk structure in engineering materials and it is expected to lead to a significant potential for exhibiting excellent mechanical properties and functionalities which extend the fields of applications of the HPT-induced hybrid materials.

For examining the feasibility of the HPT processing with the simple sample set-up for fabricating new metal systems, a further examination was conducted for producing an Al-Cu system through 10, 20 and 60 turns by HPT under 6.0 GPa at RT from the commercial purity Al and Cu. Overviews of the HPT-processed Al-Cu metal disks are shown in Figure 5(a) for 10 and 60 turns. It should be noted that at the central regions in both disks the bright regions denote the Al-rich phase and the dark regions correspond to the Cu-rich phase whereas the grey color at the overall disk edges may describe a complete mixture of Al and Cu as was demonstrated in the Al-Mg system.

There is a consistent trend of microstructural evolution between the Al-Cu and the Al-Mg systems during HPT with increasing numbers of turns. Thus, due to diffusion bonding of the Al and Cu phases, the Al-Cu disk obtained a multi-layered microstructure in a wide region from the disk center towards *r*

≈ 3-4 mm and a mixture of very fine Cu phases within the Al matrix in the remainder of the region at the disk edge after 10 HPT turns. Additional HPT through 60 turns demonstrated a significant influence to reduce the multi-layered region at the disk center to *r* <2 mm and the wide peripheral region showed a complete mixture of Al and Cu.

Representative TEM micrographs are shown in Figure 5(b) and (c) for the Al-Cu disk edges after HPT for 20 and 60 turns, respectively. Processing by HPT for 20 turns produced a layered nanostructure with an average thickness of ~20 nm where the microstructure consists of a simple mixture of the Al-rich phase with a brighter color and the Cu-rich phase with a darker color as shown in Figure 5(b). By contrast, after 60 HPT turns the Cu is completely dissolved into the Al matrix and there was no evidence of the Cu-rich phase at the disk edge. Significant grain refinement was achieved so that true nano-scale grains with an average grain size of ~30 nm were observed in an equiaxed microstructure as shown in Figure 5(c).

The Vickers microhardness was recorded at the mid-height along the disk diameters of the Al-Cu disks after HPT for 10, 20 and 60 turns and the results are shown in Figure 5(d) where the hardness of the base materials of Al and Cu after 10 HPT turns are denoted by the dashed lines at Hv ≈ 65 and ~150, respectively. The central regions of *r* <3-4 mm after 10 turns and *r* <1 mm after 60 turns where the areas hold the layered microstructure as seen in Figure 5(a) demonstrated the lower hardness values which are consistent with the hardness of the base material of Cu when processed separately by HPT for 10 turns. The hardness at the peripheral regions recorded exceptionally high hardness values of Hv ≈ 250, 400 and 500 with increasing numbers of turns to 10, 20 and 60, respectively.

These results on the Al-Cu system were obtained from preliminary examinations and further studies are necessary to investigate the detailed compositional changes through the diffusion bonding during HPT, the strengthening mechanism and the functionalities of the synthesized system after HPT. Nevertheless, the exceptionally high hardness is greater than the hardness which is achievable by grain refinement on the separate base metals and thereby it indicates the synthesis of new phases exhibiting excellent hardness in the HPT-processed Al-Cu system. Thus, the present study demonstrates a considerable potential for applying HPT processing for the synthesis of new alloy systems containing gradient-type microstructures, especially by simply and expeditiously fabricating a wide range of MMNCs from simple metals and alloys and by incorporating an additional treatment of PDA to further improve the mechanical properties of these HPT-processed materials.

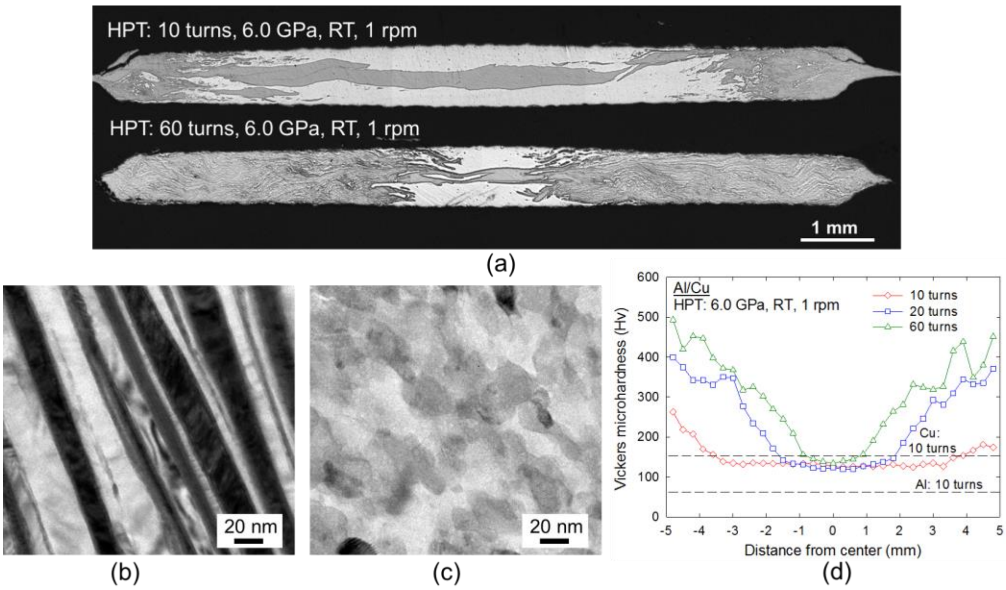

Figure 5. (a) an overview of the microstructure of the Al-Cu system after HPT for 10 and 60 turns, TEM micrographs at the disk edges of the Al-Cu system after HPT for (b) 20 turns and (c) 60 turns and (d) Vickers microhardness variations of the Al-Cu disks after HPT.

5. Summary and conclusions

The synthesis of an MMNC by forming intermetallic compounds was demonstrated in an Al-Mg system using conventional HPT processing for 20 turns at RT through the diffusion bonding. The significance of applying PDA was demonstrated by improving the strain rate sensitivity leading to an excellent potential for achieving high plasticity in the Al-Mg system. Moreover, a potential for making use of HPT at ambient temperature was demonstrated for synthesizing an Al-Cu system exhibiting exceptionally high strength after HPT through 60 turns. Additional results are now needed to confirm the feasibility of using this approach for other metallic systems.

Acknowledgements

This work was supported by the NRF Korea funded by MoE under Grant No. NRF-2016R1A6A1A03013422 and by MSIP under Grant No. NRF-2016K1A4A3914691 (MK); the NRF Korea funded by MSIP under Grant No. NRF-2015R1A5A1037627 (JIJ); and the European Research Council under ERC Grant Agreement No. 267464-SPDMETALS (TGL).

References

[1] Liddicoat PV, Liao XZ, Zhu YT, Zhao YH, Lavernia EJ, Murashkin MY, Valiev RZ and Ringer SP 2010 *Nature Commun.* **1** 63/1.
[2] Valiev RZ, Islamgaliev RK and Alexandrov IV 2000 *Prog. Mater. Sci.* **45** 103.
[3] Zhilyaev AP and Langdon TG 2008 *Prog. Mater. Sci.* **53** 893
[4] Langdon TG 2013 *Acta Mater.* **61** 7035.
[5] Zhilyaev AP, Gimazov AA, Raab GI and Langdon TG 2008 *Mater. Sci. Eng. A* **486** 123.
[6] Edalati K, Yokoyama Y and Horita Z 2010 *Mater. Trans.* **51** 23.
[7] Korznikov AV, Safarov IM, Laptionok DV and Valiev RZ 1991 *Acta Metall. Mater.* **39** 3193.
[8] Edalati K, Horita Z, Fujiwara H and Ameyama K 2010 *Metall. Mater. Trans. A* **41A** 3308.
[9] Zhilyaev AP, Ringot G, Huang Y, Cabrera JM and Langdon TG 2017 *Mater. Sci. Eng. A* **688** 498.
[10] Ahn B, Zhilyaev AP, Lee H-J, Kawasaki M and Langdon TG 2015 *Mater. Sci. Eng. A* **635** 109.
[11] Kawasaki M, Ahn B, Lee H-J, Zhilyaev AP and Langdon TG 2015 *J. Mater. Res.* **31** 88.
[12] Ahn B, Lee H-J, Choi I-C, Kawasaki M, Jang J-I and Langdon TG 2016 *Adv. Eng. Mater.* **18** 1001.
[13] Valiev RZ, Sergueeva AV and Mukherjee AK 2003 *Scripta Mater.* **49** 669.
[14] Huang Y, Lemang M, Zhang NX, Pereira PHR and Langdon TG 2016 *Mater. Sci. Eng. A* **655** 60.
[15] Shahmir H, He J, Lu Z, Kawasaki M and Langdon TG 2016 *Mater. Sci. Eng. A* **676** 294.
[16] Han J-K, Lee H-J, Jang J-i, Kawasaki M and Langdon TG 2017 *Mater. Sci. Eng. A* **684** 318.
[17] Divinski SV, Reglitz G, Rösner H, Estrin Y and Wilde G 2011 *Mater. Sci. Eng. A* **59** 1974.
[18] Lee D-H, Choi I-C, Seok M-Y, He J, Lu Z, Suh J-Y, Kawasaki M, Langdon TG and Jang J-i 2015 *J. Mater. Res.* **30** 2804.
[19] Sauvage X, Wilde G, Divinski SV, Horita Z, Valiev RZ 2012 *Mater. Sci. Eng. A* **540** 1.
[20] Lucas BN and Oliver WC 1999 *Metall. Mater. Trans. A* **30A** 601.
[21] Valiev RZ, Alexandrov IV, Zhu YT and Lowe TC 2002 *J. Mater. Res.* **17** 5.
[22] Valiev R 2002 *Nature* **419** 887.
[23] Kumar P, Kawasaki M and Langdon TG 2016 *J. Mater. Sci.* **51** 7.
[24] Zhu YT and Liao XZ 2004 *Nat. Mater.* **3** 351.
[25] Valiev RZ, Estrin Y, Horita Z, Langdon TG, Zehetbauer MJ and Zhu YT 2016 *Mater. Res. Lett.* **4** 1.
[26] Oh-ishi K, Edalati K, Kim HS, Hono K and Horita Z 2013 *Acta Mater.* **61** 3482.
[27] Bouaziz O, Kim HS and Estrin Y 2013 *Adv. Eng. Mater.* **15** 336.
[28] Qiao X, Li X, Zhang X, Chen Y, Zheng M, Golovin IS, Gao N and Starink MJ 2016 *Mater. Lett.* **181** 187.
[29] Kang JY, Kim JG, Park HW and Kim HS 2016 *Sci. Rep.* **6** 26590/1.